

Characterization of reactive DC magnetron sputtered TiAlN thin films

B. Subramanian^{*1}, K. Ashok¹, P. Kuppusami², C. Sanjeeviraja³, and M. Jayachandran¹

¹ ECMS Division, Central Electrochemical Research Institute, Karaikudi-630 006, India

² Physical Metallurgy Section, Indira Gandhi centre for Atomic research, Kalpakkam-603102, India

³ Department of Physics, Alagappa University, Karaikudi-630003, India

Received 28 January 2008, revised 9 June 2008, accepted 26 June 2008

Published online 25 July 2008

Key words thin films, reactive sputtering, XRD.

PACS 68.55-a, 81.15.cd, 61.05.cp

Thin films of about 1 μm Titanium Aluminum Nitride (TiAlN) were deposited onto mild steel substrates by reactive direct current (DC) magnetron sputtering using a target consisting of equal segments of titanium and aluminum. X-ray diffraction (XRD) analysis showed that the TiAlN phase had preferred orientations along 111 and 200 with the face-centered cubic structure. Scanning Electron Microscope (SEM) and Atomic Force Microscope (AFM) analyses indicated that the films were uniform and compact. Photoluminescence (PL) spectra reveal that TiAlN thin films are of good optical quality. Laser Raman studies revealed the presence of characteristic peaks of TiAlN at 312.5, 675, and 1187.5 cm^{-1} .

© 2008 WILEY-VCH Verlag GmbH & Co. KGaA, Weinheim

1 Introduction

Recently, light metal element, such as aluminum was incorporated into the Titanium Nitride (TiN) forming TiAlN to overcome its shortcoming of instability at high temperatures [1]. TiAlN films have been widely developed in many application fields such as cutting, forming tools, semiconductor devices, optical instruments, compressor blade of aero engines, diffusion and biocompatible barriers [2-4]. Recently TiAlN films have also been studied for applications in satellite temperature control [5]. A fundamental advantage of TiAlN films is that they form a highly adhesive, dense protective Al_2O_3 film at their surface when heated, preventing further inward diffusion of oxygen into the coated material [6].

Many studies have been reported on the deposition and properties of TiAlN coating produced by various fabrication techniques. Nanostructure and hardness of TiAlN thin films with different compositions prepared by plasma enhanced chemical vapor deposition [7] were investigated. Physical Vapor Deposition (PVD) such as Cathodic arc plasma deposition [8], Plasma assisted chemical vapor deposition [9] electron beam evaporation [10], arc ion plating [11], reactive DC magnetron sputtering [12] and combined cathodic steered arc etching/unbalanced magnetron sputtering [13]. Higher cutting speed can be obtained with TiAlN coating, by decreasing the thermal loading of the substrate [14]. The improved hardness and better cutting performance especially in higher cutting speed range of the film, deposited by reactive DC magnetron sputtering, have been attributed to shrinkage in the lattice parameters caused by the replacement of larger titanium atoms by smaller aluminium atoms [15]. In this investigation, the structural properties of DC magnetron sputtered TiAlN films on mild steel substrates are reported.

2 Experimental

The layers of TiAlN were deposited on well-cleaned mild steel (MS) substrates using a DC magnetron sputter deposition unit HIND HIVAC. The base vacuum of the chamber was below 10^{-6} Torr and the substrate

* Corresponding author: e-mail: tpsenthil@yahoo.com

temperature was kept at 400°C. High purity argon was fed into the vacuum chamber for the plasma generation. The substrates were etched for 5 min at a DC power of 50 W and an argon pressure of 10mTorr (1.33Pa). The deposition parameters for TiAlN sputtering are summarized in table 1.

Table 1 Deposition parameters for TiAlN reactive sputtering.

Objects	Specification
Target (2" Dia)	Ti (99.9 %), Al (99.9%)
Substrate	Mild steel
Target to substrate distance	60 mm
Ultimate vacuum	1×10^{-6} mbar
Operating vacuum	2×10^{-3} mbar
Sputtering gas (Ar: N ₂)	1: 1
Power	250 Watt
Substrate temperature	400 °C

X-ray analysis was conducted in PANalytical-X'Pert Pro using CuK α (1.514Å) with the θ -2 θ scan mode and a thin film attachment with a parallel plate collimator 0.18°. The surface morphology of the coating was studied by SEM using a Hitachi S 3000H microscope equipped with EDS. The topography of the films was examined using molecular imaging AFM. Micro hardness of the films on mild steel was evaluated by using a DM-400 micro hardness tester from LECO with Vickers indenters. A dwelling time of 15 s and a load of 25 g and 5 g were used for the measurement. The excitation wavelength was 632.8 nm for Raman measurements. The data were collected with a 10 s data point acquisition time in the spectral region of 200-1200 cm⁻¹. The PL measurements were made using a Cary Eclipse Fluorescence Spectrophotometer (VARIAN) employing PbS photo-detector and a 150 W Xe arc discharge lamp as the excitation light source.

3 Results and discussion

Structural analysis The thermal stability of TiAlN was found by annealing the films coated on mild steel heated in atmospheric air in a resistive furnace at the temperatures of 500°C, 600°C, 700°C and 800°C. The desired annealing temperature was maintained for 30 min with a slow heating rate of 3 K/min and subsequently the samples were cooled down at the same rate.

The XRD patterns obtained for the reactive magnetron sputter deposited TiAlN films on MS with the Ar/N₂ ratio of 1:1 indicated that the successful formation of TiAlN films with face-centred cubic (fcc) crystal system. The structural changes of the film as a result of annealing were analyzed. The observed 'd' values are in very good agreement with standard JCPDS No: 37-1140. The peak at 37.7°, 43.8° and 63.9° corresponds to diffraction along 111, 200 and 222 planes with the standard deviation of 2.6.

The position of preferred orientation from 200 was found to shift slightly towards higher angle at 800°C as shown in figure 1. The grain size of the annealed TiAlN films was determined from the full width at half maximum (FWHM) of the X-ray diffraction peak 200 using Scherrer's equation [16] $D = 0.9 \lambda / \beta_{20} \cos \theta$.

Where λ is the wavelength of the X-ray, θ is the Bragg's angle and β_{20} is the FWHM of 200 peak of the XRD pattern. Figure 2 shows the grain size increase on the annealing temperature up to 700°C. An increase in thermal energy leads to an increase in the adatom mobility and hence a larger grain size. The grain size falls steeply above 700°C, which may be due to the instability at higher temperature and rapid decrease of surface energy with crystalline growth [17]. The number of crystallites/ unit area (N) is found out from $N = t/D^3$ where t is the thickness of the thin film and D is the grain size, which will elucidate the nature of the prepared TiAlN films.

The origin of the strain is related to the lattice misfit, which in turn depends upon deposition conditions. The strain (ϵ) and dislocation density (δ) developed in the TiAlN films were evaluated from the relation $\epsilon = (\beta_{20} \cos \theta) / 4$ and $\delta = n / D^2$ [18], where β_{20} is the FWHM of 200 peak, D is the grain size and n is a factor, which equals unity for thin films [19]. The strain and dislocation density decreases and then increases above 700°C as shown in figure 3. The decrease in dislocation density indicates the formation of high-quality films at higher annealing temperatures. The dislocations get more thermal energy and have a higher mobility. It leads to the reduction in the concentration of lattice imperfections. Thus, there is a decrease in the density of nucleation centers, and under these circumstances a smaller number of centers start to grow [20]. At the same time, on increasing the temperature the films gets oxidized completely and peel off occurs above 700°C.

The variation of lattice constant with annealing temperature is shown in figure 4. The calculated lattice constants ($\approx 4.14\text{\AA}$) are found to agree with the values reported in the literature ($a = 4.17\text{\AA}$) [21]. The lattice constant increases with the annealing temperature and then start to decrease at 700°C . The change in lattice constant may be due to the film grains are strained and that may be owing to the change of nature and concentration of the native imperfections [22]. The average internal stress developed in the film is determined by the relation $\sigma = (E/2\gamma) (a_0 - a)/a_0$ [23], where a_0 is the bulk lattice constant of TiAlN and 'a' refers to the lattice constant perpendicular to the film plane.

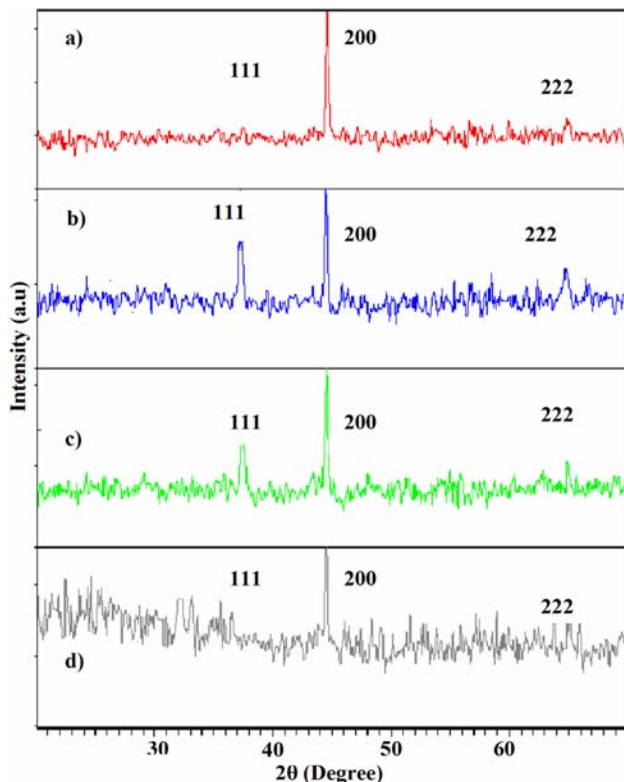


Fig. 1 XRD pattern of the sputtered TiAlN film on mild steel at different annealing temperatures a) 500°C b) 600°C c) 700°C d) 800°C . (Online color at www.crt-journal.org)

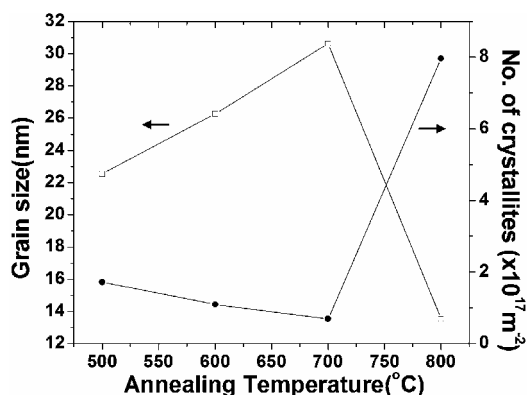


Fig. 2 Variation of grain size and number of crystallites with annealing temperature. The estimated standard deviation for the grain size and number of crystallites was 0.45 and 0.95 respectively.

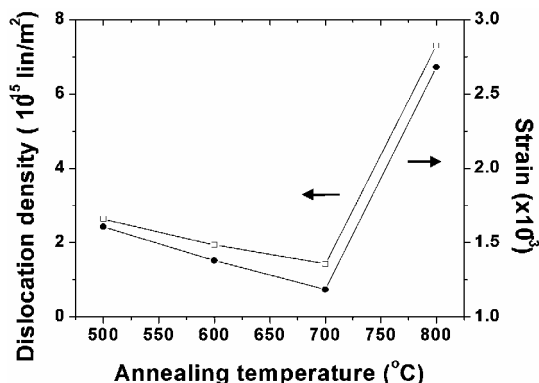


Fig. 3 Variation of dislocation density and strain with annealing temperature. The estimated standard deviation for the dislocation density and strain was 0.8 and 0.25 respectively.

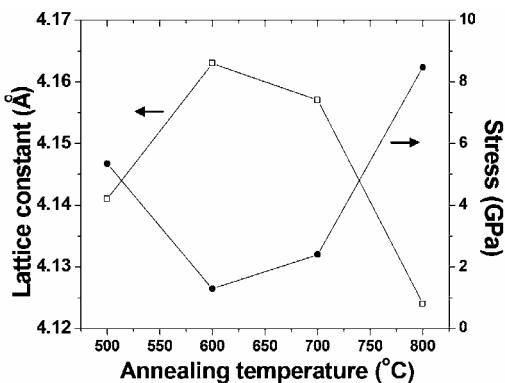


Fig. 4 Variation of lattice constant and stress with annealing temperature. The estimated standard deviation for the lattice constant and stress was 0.01 and 1.02 respectively.

Young's modulus and Poisson's ratio for the bulk TiAlN were $E = 215$ GPa and $\gamma = 0.14$ respectively. Internal residual stresses could be built up in the deposited films due to lattice mismatch between the film structure and the substrate surface. The behavior of residual stress with respect to annealing temperature is shown in figure 4. TiAlN films deposited at 400°C exhibited a compressive stress. During annealing the residual stress reached a minimum at 600°C and turned tensile stress at 700°C . This tensile stress is responsible for the formation of micro-blisters, which could be considered as the incomplete rearrangement of defects during annealing process.

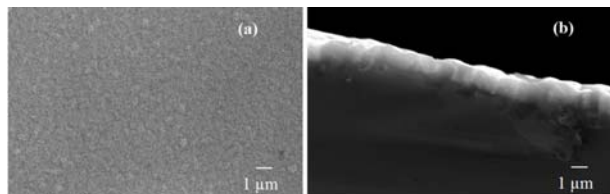


Fig. 5 SEM picture of TiAlN film on MS a) Plane view b) Cross sectional view.

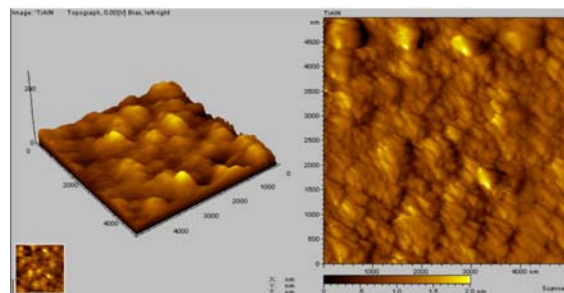


Fig. 6 AFM image showing the topography of TiAlN film on mild steel. (Online color at www.crt-journal.org)

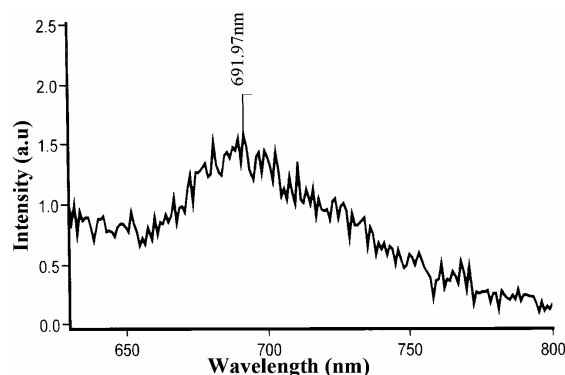


Fig. 7 PL emission spectrum obtained for magnetron sputtered TiAlN film.

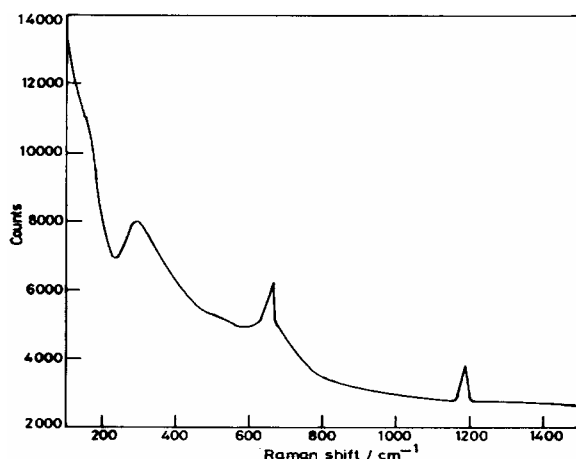


Fig. 8 Laser Raman Spectrum obtained for TiAlN thin film.

Micro structural analyses The surface was homogeneous and dense as observed from the plane view of the TiAlN thin film is as shown in figure 5a. The columnar structure can be seen from the cross sectional SEM picture of the TiAlN coated steel as shown in figure 5b. The surface topography of these TiAlN thin films was also studied using AFM for a scanned area of $5 \times 5 \mu\text{m}$ is shown in figure 6. The columnar structure is observed. PVD films show an open columnar structure of the zone 1 type according to the structure model of [24]. From the horizontal cross section analysis, the minimum and maximum grain size was estimated to be in the range of 200 to 250 nm and some shallow valleys of around 40 nm depths were observed. The value of the mean roughness R_a was calculated as the deviations in height from the profile mean value [25]. The value estimated from these images was approximately 8.6 nm with the standard deviation of 0.01.

Although the detection efficiency of low atomic mass number elements such as nitrogen is low in EDS analysis the relative compositions of TiAlN films were found to be 36.22 % for Ti, 29.30 % for Al, 33.08 % for N, 0.71 % for Ar and 0.69 % for O with the standard deviation of 1.69. In addition to constituent elements traces of argon and oxygen were also detected in the EDS data. In situ Ar^+ ion bombardment of the growing film could be reason for the incorporation of Ar and Oxygen could be because of very thin Oxide layer formed on the surface of the film. It may also be due to an incipient corrosion process during handling the sample. The surface microhardness values of TiAlN films on steel were measured using a Vickers diamond indenter at a

load of 10 g and 25 g for 15 s. The mean values, 2700 HV 0.01 and 2560 HV 0.025 were calculated with the standard deviation of 8.6. Nearly the same values were found for all the samples.

Photoluminescence and laser Raman studies PL spectrum recorded at room temperature for the TiAlN film is shown in figure 7. It is interesting to note that emission appearing at 691.97 nm for the excitation at 346 nm is only in the visible region. This implies that the TiAlN films prepared by DC reactive magnetron sputtering are of good optical quality. The characteristic peaks at 312.5, 675, and 1187.5 cm^{-1} , related to transverse acoustic (TA) / longitudinal acoustic (LA), transverse optical (TO) / longitudinal optical (LO) and second order optical (2O) modes of TiAlN, respectively, were observed in the Raman spectra of TiAlN films (Fig. 8) prepared by reactive sputtering process. This is in good agreement with the reported values for TiAlN films by [26].

4 Conclusions

TiAlN coating was successfully deposited on mild steel and the material properties were investigated. The structural analysis using XRD reveals that the films are polycrystalline in nature possessing fcc structure and having the lattice parameter a of about 4.14 Å. The observed Raman peaks confirmed the formation of TiAlN films. A dense columnar structure was observed from SEM analysis. The good optical quality of these films was observed from PL studies.

Acknowledgements One of the authors (B.S) thanks the Department of Atomic Energy (DAE), Board of Research in Nuclear Sciences (BRNS), Mumbai, for a research grant (Sanction No. 2006/37/37/BRNS/2068).

References

- [1] P. W. Shum, W. C. Tam, K. Y. Li, Z. F. Zhou, and Y. G. Shen, *Wear* **257**, 1030 (2004).
- [2] M. C. Kang, I. W. Park, and K. H. Kim, *Surf. Coat. Technol.* **163-164**, 734 (2003).
- [3] S. D. Kim, L. S. Hwang, J. K. Rhee, T. H. Cha, and H. D. Kim, *Electrochem. Solid-State Lett.* **4**, G7 (2001).
- [4] M. Hock, E. Schaffer, W. Doll, and G. Kleer, *Surf. Coat. Technol.* **163**, 689 (2003).
- [5] M. Brogren, G. L. Harding, R. Karmhag, C. G. Ribbing, G. A. Nikasson, and L. Stenmark, *Thin Solid Films* **370**, 268 (2000).
- [6] K. Chakrabarti, J. J. Jeong, S. K. Hwang, Y. C. Yoo, and C. M. Lee, *Thin Solid Films* **406**, 159 (2002).
- [7] J. Sheih and M. H. Hon, *Thin Solid films* **391**, 101(2001).
- [8] Kwang-Lung Len, Ming-Yeng Hwang, and Cheng-Dauwel, *Mat. Chem. Phys.* **46**, 77 (1996).
- [9] D. Munz, *J. Vac. Sci. Technol. A* **4**, 2695 (1986).
- [10] J. Aromaa, H. Ronkainen, A. Mahiout, and S. P. Hannula, *Surf. Coat. Technol.* **49**, 353 (1991).
- [11] A. Kiruma, T. Murakami, K. Yamada, and T. Suzuki, *Thin Solid Films* **382**, 101 (2001).
- [12] C. Kulwantsingh, A. K. Grover, K. Totlani, and A. K. Suri, *Trans IMF* **79**, 5 (2001).
- [13] D. B. Lewis, S. Creasy, Z. Zhou, J. J. Forsyth, A. P. Ehiasarian, P. Hovsepian, Eh, Q. Luo, W. M. Rainforth, and W. D. Munz, *Surf. Coat. Technol.* **177**, 252 (2004).
- [14] K. N. Andersen, E. J. Bienk, K. O. Schweitz, and H. Reitz, *J. Chevallier, Surf. Coat. Technol.* **123**, 219 (2003).
- [15] D. B. Lewis, L. A. Donohue, M. Lembke, W. D. Munz, R. Kuzel, V. Valvoda, and C. Blomfield, *Surf. Coat. Technol.* **114**, 187 (1999).
- [16] B. D. Cullity, "Elements of X-ray diffraction", MA: Addison-Wesley, 1972.
- [17] Godhuli Sinha, Kalyan Adhikary, and Subhadra Chaudhuri Opt. Mater. **29**, 718 (2007).
- [18] G. B. Williamson and R. C. Smallman, *Phil. Mag.* **1**, 34 (1956).
- [19] V. Senthilkumar, S. Venkatachalam, C. Viswanathan, S. Gopal, Sa. K. Narayandass, D. Mangalaraj, K. C. Wilson, and K. P. Vijayakumar, *Cryst. Res. Technol.* **40** 573 (2005).
- [20] T. S. Li, H. Li, and F. Pan, *Surf. Coat. Tech.* **137**, 225 (2001).
- [21] Albano Cavaleiro and Jeff Th. M. De. Hosson, "Nano structured coatings", New York: Springer, 2006, p. 184.
- [22] P. K. R. Kalita and B. K. Sarma, *Bull. Mater. Sci.* **23**, 313 (2000).
- [23] K. L. Chopra, "Thin film phenomena", New York: McGraw Hill, 1969, p. 270.
- [24] W. Thornton, *J. Vac. Sci. Technol. A* **4**, 2309 (1986).
- [25] M. H. Jacobs, *Surf. Coat. Tech.* **29**, 221 (1986).
- [26] C. P. Constable, J. Yarwood, and W. D. Münz, *Surf. Coat. Tech.* **116**, 155 (1999).